Volume 1 | Number 1 | Jan 2013 | Pages 1–100

ChemComm

Chemical Communications
www.rsc.org/chemcomm

ROYAL SOCIETY OF CHEMISTRY

This is an *Accepted Manuscript*, which has been through the Royal Society of Chemistry peer review process and has been accepted for publication.

Accepted Manuscripts are published online shortly after acceptance, before technical editing, formatting and proof reading. Using this free service, authors can make their results available to the community, in citable form, before we publish the edited article. We will replace this *Accepted Manuscript* with the edited and formatted *Advance Article* as soon as it is available.

You can find more information about *Accepted Manuscripts* in the **Information for Authors**.

Please note that technical editing may introduce minor changes to the text and/or graphics, which may alter content. The journal's standard **Terms & Conditions** and the **Ethical guidelines** still apply. In no event shall the Royal Society of Chemistry be held responsible for any errors or omissions in this *Accepted Manuscript* or any consequences arising from the use of any information it contains.

Journal Name

COMMUNICATION

Growth of filament under macromolecular confinement by scaling theory

Lin Zhu,[a] Wei Pan,[a] Xi Lu,[b] Desheng Li,[b] Jiang Zhao*[b] and Dehai Liang*[a]

Quantitatively describing the macromolecular confinement is still a challenge. Using the assembly of DNA tiles in polyacrylamide network as a model, we studied the effect of macromolecular confinement on the growth of filament by scaling theory. Results show that the confinement regulates the morphology, the initial growth rate v, and the eventual length of the filament N_m. The initial growth rate is dependent on the medium viscosity η as $v \propto \eta^{-0.94}$, and the filament adjusts its length in the given confined space as $N_m \propto \left(\xi/R_g\right)^{1.8}$, with ξ being the mesh size of the polyacrylamide solution and R_g being the radius of gyration of polyacrylamide.

The congested interior of a living cell generates significant impacts on the structure and reactivity of biomacromolecules, such as protein[1], DNA[2, 3], peptide[4, 5] and liposome[6]. Experimental and computational studies have demonstrated that macromolecular crowding and confinement are two fundamental effects, with the former favouring the process of increasing the available volume, such as the formation of more compacted conformation of proteins[7-10] and nucleic acid chains[2], the binding of macromolecules to one another[3, 11], the formation of aggregates like amyloids[12-15], actin[16] and microtubule[17], while the latter may have complex effects depending on the relative size and shape of the product and the confining volume[18, 19]. Both the effects are accountable for the big differences of the behaviours observed *in intro* and those occurring *in vivo* [20-22]. However, quantitatively describing the macromolecular crowding and confinement effect is still a challenge. On one hand, the cells contain many proteins, complex sugars, and nucleic acids, with the total volume ratio being up to 40% [23]. It is difficult to build a simple model to simulate such heterogeneous system. On the other hand, the specific and other non-specific interactions between the target molecules and the crowding environment[24] conceal or alter the macromolecular crowding and confinement effect which is driven purely by entropy and can be attributed to excluded volume interactions.

From the viewpoint of polymer physics, the congested cell interior can be treated as concentrated polymer solution. The movement of individual polymer under such conditions is restricted in a "Tube" as proposed by Doi and Edward [25]. The diffusion of small molecules is also affected by the pore size (or correction length) of the transient polymer network [26]. The diameter of the "Tube" or the pore size of the polymer network, which defines the degree of confinement, can be described by a scaling relationship with the concentration of polymer solution[18, 27]. Therefore, the scaling theory should be applicable to the effect of macromolecular crowding and confinement. Computer simulation has demonstrated that the protein folding temperature showed a scaling relationship with the size of confining space[28]. To validate the scaling relationship by experiments, the targeting molecules should have no specific or other non-specific interactions with the crowding medium. The development of DNA nanotechnology provides a practical approach to fabricate well-defined nano-structures with desirable shape and topology [29, 30]. Many water soluble polymers, such as polyacrylamide (PAM) and polyvinylpyrrolidone (PVP) [31, 32], do not have specific or non-specific interactions with DNA. Herein, we chose DNA filament as the object, and studied its assembly in PAM network.

The DNA filament is assembled by five DNA strands [33, 34], whose sequences are listed in Fig. 1 A. These DNA strands form a rectangular tile of 4×2×14.3 nm. Four to ten of such tiles can further assemble in circumference into a tubing filament with a diameter ranging from 7 to 20 nm[33]. One of the five DNA strands (strand 5th) is labelled by a fluorophore, Alex 532, allowing a real time observation of the assembly process by fluorescent microscopy. The growth of the DNA filament is confined in the network formed by concentrated PAM solution. The molecular mass (M_w) and radius of gyration (R_g)

a. *Beijing National Laboratory for Molecular Sciences and the Key Laboratory of Polymer Chemistry and Physics of Ministry of Education, College of Chemistry and Molecular Engineering, Peking University, Beijing 100871, P. R. China*
E-mail: dliang@pku.edu.cn
b. *Beijing National Laboratory for Molecular Sciences, Institute of Chemistry, Chinese Academy of Sciences, Beijing 100190, P.R. China*
E-mail: jzhao@iccas.ac.cn

Electronic Supplementary Information (ESI) available: The experimental materials, methods, and movies. See DOI: 10.1039/x0xx00000x

COMMUNICATION

Journal Name

of PAM are 5.1×10^6 g/mol and 101 nm, respectively. The overlap concentration *C** is calculated to be 2.0 mg/ml according to $C^*=M_w/(4\pi N_A R_g^3/3)$, with N_A being the Avogadro's number. At concentrations above *C**, the polymer chains penetrate and entangle with each other to form a resilient and dynamic network. The pore size ξ of the network can be fine tuned by varying the concentration according to $\xi = R_g (C/C^*)^{-0.76}$. [26] To ensure that the DNA filaments are properly confined and the crowding effect is negligible, we choose 10 mg/mL, five times higher than *C**, as the lowest polymer concentration. The pore size is about 30 nm under such conditions. Total Internal Reflection Fluorescence Microscopy (TIRFM) was used to in situ monitor the assembling of DNA tiles at varying PAM concentrations. The dynamics and topology of the assembly can be obtained simultaneously from the video recorded in TIRFM [35, 36].
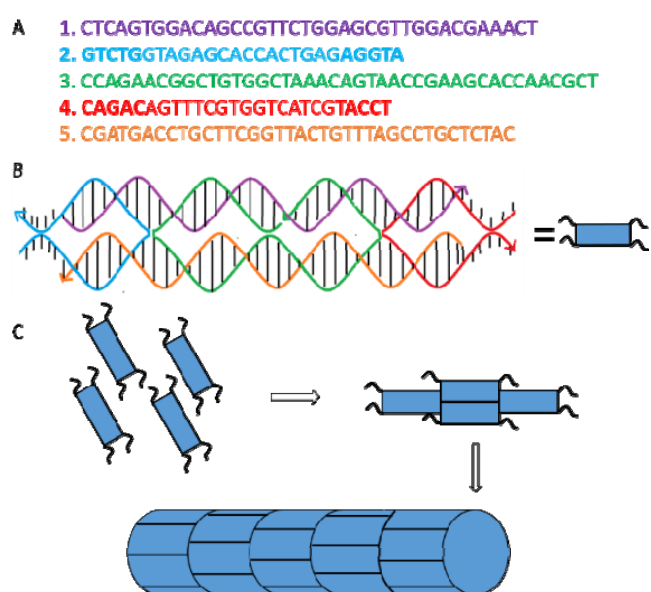
FIG. 1. (A) The sequence of the DNA strands; (B) the DNA tile formed by strands; (C) the assembly of DNA filament by the tiles.

Figure 2 compares the real-time TIRFM images of DNA filament at different PAM concentrations. Pure solvent (0 mg/mL PAM) is used as the control. Without the confinement of polymer network, the DNA tiles diffuse very fast at the beginning. They can assemble into filaments with time, but these filaments quickly stick with each other to form branched structures (Fig. 2A1-2A4). Eventually, the branched structures further connect into a network, whose overall diffusion rate is slow. However, the branches dangling outside the network still swing back and forth at a fast rate as shown in movie S1 [37]. The growth of one dimensional DNA filament is significantly improved when DNA tiles are confined in 10 mg/mL PAM. As shown in Fig. 2B1, the length of the DNA filament increases much faster than that without confinement. The growth at this stage is mainly via the attachment of individual DNA tile at the ends of the filament. Once the length of the filament reaches certain level, different filaments start to bind together via end to end connection as shown in movie S2 [38]. The end to side

connection, which leads to branched structures, is also observed (Fig. 2B1-2B4). This suggests that the originally formed filaments have defects, which is in agreement with our previously findings [39]. The confinement effect becomes stronger at higher PAM concentrations. As shown in Fig. 2C-2E, both the growth rate and the length of the DNA filaments decrease with increasing PAM concentration, indicating that a stronger confinement prevents the DNA tiles from assembling into longer filaments. On the other hand, the branching of DNA filaments is also significantly suppressed as the PAM concentration increases. The enhancement on the growth in one-dimension is in agreement with our previously findings. This result also matches the prediction of the "Tube" model proposed by Doi and Edward [25]. As shown in Fig. 2E1-E4, No branching is observed in the studied time periods at 30 mg/mL PAM. This is reasonable considering that each DNA filament is "trapped" in the network. It can only diffuse axially to a small extent. The lateral movement is strongly suppressed, especially for the longer ones as shown in movie S3 [40]. No prominent change in filament diameter is observed from TIRFM and TEM images (Fig. S1) at the studied conditions.
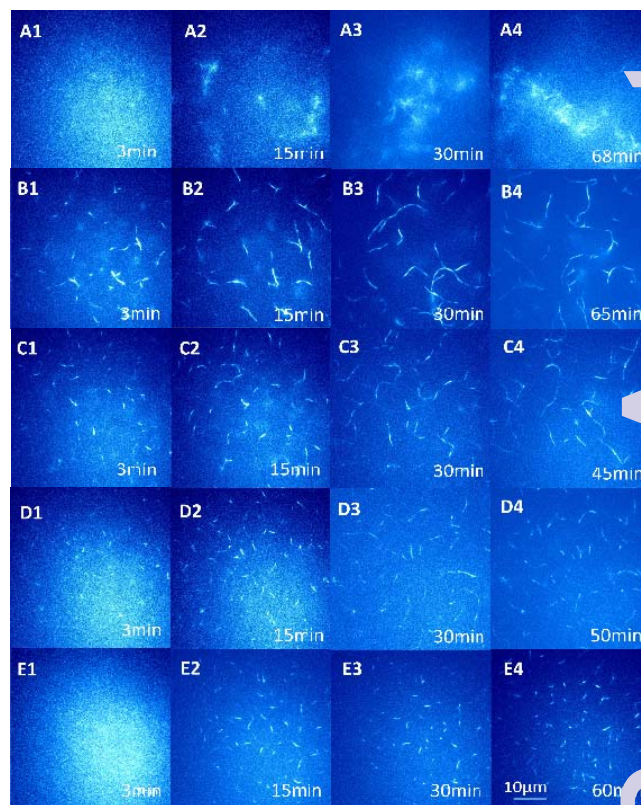
FIG. 2. Video images showing the growth of DNA filament in PAM matrix of varying concentrations (A-E) at selected time points (1-4). The concentration of PAM: (A) 0 mg/ml, (B) 10 mg/mL, (C) 15 mg/mL, (D) 20 mg/mL, (E) 30 mg/mL. The concentration of each DNA strand is 100 nM. The dimension of each panel is 50 × 50 µm. A larger view is attached as Figure S2.

To build a scaling relationship between the confinement effect and the assembly of DNA tiles, we measured the length of the DNA filament at selected time points by software ImageJ

Journal Name

COMMUNICATION

Figure 3 compares the results at around 50 min, at which time period the growth of DNA filament is not prominent. At 10 mg/mL PAM, the length of the filament ranges from 2 μm to more than 20μm, with the average value being 7.9 ± 4.5 μm (Fig. 3A). At 15 mg/mL PAM, the broad distribution remains, but the averages value decreases to 5.9 ± 4.4 μm (Fig. 3B). With further decreasing concentration to 20 mg/mL, the length distribution becomes narrower, and the average length drops to 3.9 ± 1.8 μm (Fig. 3C). It further decreases to 1.6 ± 0.6 μm at 30 mg/mL PAM (Fig. 3D). The length distribution is also the narrowest at the studied conditions.
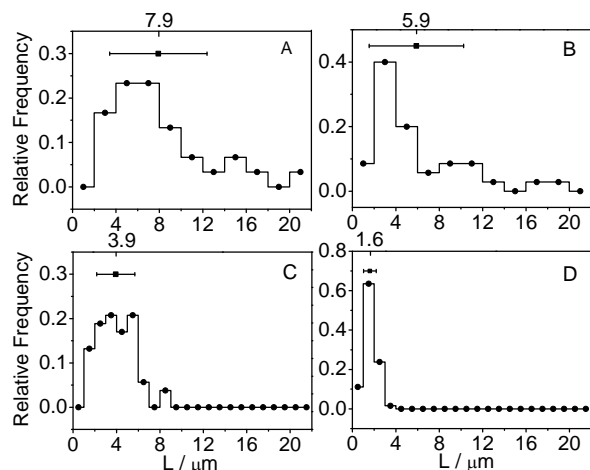
FIG. 3. The length histogram of DNA filaments after 50 min at PAM concentrations of (A) 10, (B) 15, (C) 20, and (D) 30 mg/mL.

The kinetic growth curve is obtained by using the calculated length L at different time points. As shown in Fig. 4A, the growth of DNA filaments in PAM network follows a similar pattern at the concentrations from 10 mg/mL to 30 mg/ml. All the curves can be fitted by an exponential growth equation,

$$L = L_m \left(1 - exp\left(-\frac{t}{\tau}\right)\right) \quad (1)$$

with L_m and τ being the maximum length and the characteristic growth time, respectively. The fitting results of L_m and τ at different PAM concentrations are listed in Fig. 4B. The DNA tiles can assemble into a tube of 7.9 μm when confined in 10 ml/mL PAM, but only 1.9 μm when the PAM concentration increases to 30 mg/mL. The τ values range from 10 to 13 min, and do not exhibit prominent dependence on PAM concentration, indicating that the growth is diffusion-limited [41]. Fig. 4A also shows that the growth rates ν of DNA filaments at the early stage are different. It is 0.72 μm/min in 10 mg/mL PAM. But it drops to 0.17 μm/min in 30 mg/mL PAM, by a factor of 4. Since the hydrogen bonding between DNA tiles is strong at room temperature, the assemble rate at early stage is controlled to a large extent by the diffusion of DNA tiles. The diffusion coefficient is inversely proportional to the solvent viscosity according the Stokes-Einstein equation $D = kT/6\pi\eta R$, with η being the viscosity and R being the size of the diffusion particle. Since the size of the DNA tile is comparable to the mesh size in the studied concentration, the viscosity of the medium should be used when calculating the

diffusion coefficient [26]. The measured viscosities of PAM at different concentrations are listed in Fig. 4B. The fitting of ν vs η curve (Fig. 4D) yields a power law relationship of $v \propto \eta^{-0.94}$. The exponent is close to 1, suggesting that the growth at early stage is controlled mainly by diffusion.
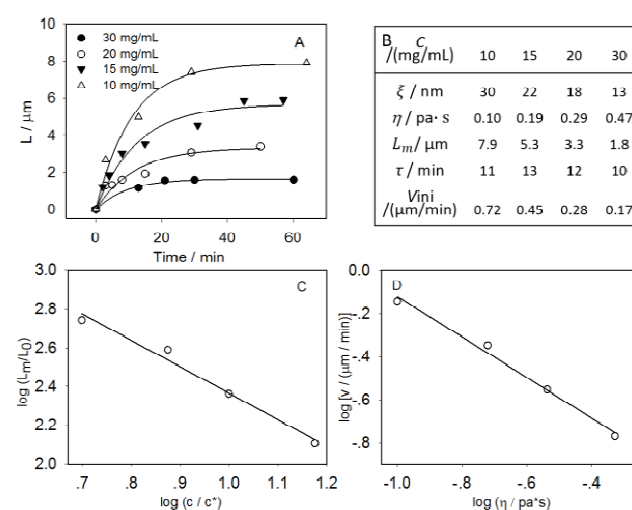
FIG. 4. Growth curve of DNA filaments at varying PAM concentrations (A). The solid lines show the fittings by using exponential growth model; Mesh size, viscosity and the fitting results (B); The dependence of L_m/L_0 on C/C^* and the power fitting curve (C); The dependence of ν on η and the power fitting curve (D).

L_m can be treated as the equilibrium length of DNA filament under confinement. Since the length of each DNA tile (L_0) is 14.3 nm, L_m/L_0 represents the maximum aggregation number N_m. It has a scaling relationship with PAM concentration. Figure 4C shows the fitting of the L_m/L_0 vs C/C^* data by a power law, which yields

$$L_m/L_0 = 4.0 \times 10^3 (C/C^*)^{-1.4} \quad (2)$$

The mesh size of the network also has a power law with the polymer concentration as mentioned above as $\xi/R_g \propto (C/C^*)^{-0.76}$. Combining this equation and equation (2) together:

$$L_m/L_0 \propto \left(\xi/R_g\right)^{1.8} \quad (3)$$

or

$$\xi/R_g \propto N_m^{0.56} \quad (4)$$

Confinement occurs at $\xi < R_g$ in the network formed by polymer solution. Therefore, the ξ/R_g ratio defines the degree of confinement in polymer network. Equation (3) shows that the length of DNA filament has a power law relationship with the degree of confinement with the exponent being 1.8. This scaling relationship can also be expressed from the viewpoint of aggregation number. As shown in Eq. (4), DNA filaments adjust its aggregation number to fit in a given confined space ξ/R_g. Interestingly, the exponent is close to 0.6 (or 0.588), suggesting that the DNA filament in PAM network follows the behaviour of coiled polymer chain in good solvent [42]. However, DNA filament is a rigid rod. Its size $R_F \propto N^1$ in non-disturbing

state. The specific behaviour of DNA filament in a confined network could be explained by the "Tube" model proposed by Doi and Edwards.[11] The "Tube" composed by PAM chains follows a similar behaviour as a flexible polymer chain. Therefore, the assembly of DNA tiles in polymer network follows the profile of a "Tube", especially at early stage. As the rigid DNA filament reaches a certain length, it has the capacity to "reset" the confining "Tube". The overall scaling relationship can be described by Eq. (3) or (4). It has been reported that a protein or polymer chain is to scale with the confining size, with an exponent being 5/3 and 15/4 in weak confinement regime or strong confinement regime, respectively.[28, 43] The scaling relationship in our work suggests that the confinement provided by transient polymer network falls into the weak confinement regime.

In summary, the confinement of polymer network shows profound effect on the growth of DNA filament. Our study demonstrated that the confinement has the capacity to regulate the growth of filaments in one-dimension, suppressing the formation of branches. The growth rate at early stage is controlled by the diffusion of DNA tiles, while at later stage, end-to-end connection is the major growth pattern. The length of DNA filaments has a power law relationship with the degree of confinement. The DNA filament has a tendency to follow the behaviours of the confining polymer chains. Since DNA filament and PAM have no specific interactions, our findings should be also applicable to the growth of other filament in a confining network purely by excluded volume interactions.

Acknowledgement

Notes and references

1   I. Kuznetsova, K. Turoverov and V. Uversky, *Int. J. Mol. Sci.*, 2014, **15**, 23090.
2   S. Nakano, D. Miyoshi and N. Sugimoto, *Chem. Rev.*, 2014, **114**, 2733-2758.
3   B. Akabayov, S. R. Akabayov, S.-J. Lee, G. Wagner and C. C. Richardson, *Nat. Commun*, 2013, **4**, 1615.
4   B. Gaharwar, S. Gour, V. Kaushik, N. Gupta, V. Kumar, G. Hause and J. K. Yadav, *Protein Peptide Lett.*, 2015, **22**, 87-93.
5   J. S. Rao and L. Cruz, *J. Phys. Chem. B*, 2013, **117**, 3707-3719.
6   Y. Liu, L. Zhu, J. Yang, J. Sun, J. Zhao and D. Liang, *Langmuir*, 2015, **31**, 4822-4826.
7   A. Samiotakis and M. S. Cheung, *J. Chem. Phys.*, 2011, **135**.
8   Y.-C. Tang, H.-C. Chang, A. Roeben, D. Wischnewski, N. Wischnewski, M. J. Kerner, F. U. Hartl and M. Hayer-Hartl, *Cell*, 2006, **125**, 903-914.
9   P. McPhie, Y. S. Ni and A. P. Minton, *J. Mol. Biol.*, 2006, **361**, 7-10.
10 Y. S. Ni, A. P. Minton and P. McPhie, *Biophys. J.*, 2004, **86**, 85a-86a.
11 M. Alcorlo, M. Jimenez, A. Ortega, J. M. Hermoso, M. Salas, A. P. Minton and G. Rivas, *J. Mol. Biol.*, 2009, **385**, 1616-1629.
12 B. Ma, J. Xie, L. Wei and W. Li, *Int. J. Biol. Macromol.*, 2013, **53**, 82-87.
13 L. A. Munishkina, E. M. Cooper, V. N. Uversky and A. L. Fink, *J. Mol. Recognit.*, 2004, **17**, 456-464.
14 L. Breydo, K. D. Reddy, A. Piai, I. C. Felli, R. Pierattelli and V. N. Uversky, *BBA-Proteins Proteom*, 2014, **1844**, 346-357.
15 D. M. Hatters, A. P. Minton and G. J. Howlett, *J. Biol. Chem.*, 2002, **277**, 7824-7830.
16 C. Rosin, P. H. Schummel and R. Winter, *Phys. Chem. Chem. Phys.*, 2015, **17**, 8330-8337.
17 M. Wieczorek, S. Chaaban and G. J. Brouhard, *Cell. Mol. Bioeng.*, 2013, **6**, 383-392.
18 A. P. Minton, *Biophys. J.*, 1992, **63**, 1090-1100.
19 J. H. Tian and A. E. Garcia, *J. Am. Chem. Soc.*, 2011, **133**, 15157-15164.
20 Y. Takaoka, Y. Kioi, A. Morito, J. Otani, K. Arita, E. Ashihara, M. Ariyoshi, H. Tochio, M. Shirakawa and I. Hamachi, *Chem. Commun.*, 2013, **49**, 2801-2803.
21 R. J. Ellis and A. P. Minton, *Nature*, 2003, **425**, 27-28.
22 A. P. Minton, *Curr. Biol.*, 2006, **16**, R269-R271.
23 S. B. Zimmerman and S. O. Trach, *J. Mol. Biol.*, 1991, **222**, 599-620.
24 I. M. Kuznetsova, B. Y. Zaslavsky, L. Breydo, K. K. Turoverov and V. N. Uversky, *Molecules*, 2015, **20**, 1377-1409.
25 M. Doi and S. F. Edwards, *The Theory of Polymer Dynamics*, Clarendon Press, Oxford, 1986.
26 I. Kohli and A. Mukhopadhyay, *Macromolecules*, 2012, **45**, 6143-6149.
27 M. Rubinstein and R. H. Colby, *Polymer Physics*, Oxford University, Oxford, 2003.
28 J. Mittal and R. B. Best, *P. Natl. Acad. Sci. USA*, 2008, **105**, 20233-20238.
29 N. C. Seeman, *Annu. Rev. Biophys. Biomol. Struct.*, 1998, **27**, 225-248.
30 N. C. Seeman, *Mol. Biotechnol.*, 2007, **37**, 246-257.
31 Q. F. Gao and E. S. Yeung, *Anal. Chem.*, 1998, **70**, 1382-1388.
32 L. G. Song, T. B. Liu, D. H. Liang, D. F. Fang and B. Chu, *Electrophoresis*, 2001, **22**, 3688-3698.
33 P. W. K. Rothemund, A. Ekani-Nkodo, N. Papadakis, A. Kumar, D. K. Fygenson and E. Winfree, *J. Am. Chem. Soc.*, 2004, **126**, 16344-16352.
34 A. Ekani-Nkodo, A. Kumar and D. K. Fygenson, *Phys. Rev. Lett.*, 2004, **93**.
35 J. R. Kuhn and T. D. Pollard, *Biophys J*, 2005, **88**, 1387-1402.
36 R. F. Hariadi, B. Yurke and E. Winfree, *Chem. Sci.*, 2015, **6**, 2252-2267.
37 See Supplemental Material for the movie S1. The real total time is 10s, the size of the screen is 39μm×29μm.
38 See Supplemental Material for the movie S2. The real total time is 460s, the size of the screen is 31 μm× 23 μm.
39 L. Niu, X. Yang, J. Zhou, C. Mao, H. Liang and D. Liang, *Chem. Commun.*, 2015, **51**, 7717-7720.
40 See Supplemental Material for the movie S3. The real total time is 404s, the size of the screen is 31 μm× 23 μm.
41 A. Magno, A. Caflisch and R. Pellarin, *J. Phys. Chem. Lett.*, 2010, **1**, 3027-3032.
42 P. Flory, *Principles of Polymer Chemistry*, Cornell University, New York, 1953.
43 T. Sakaue and E. Raphaël, *Macromolecules*, 2006, **39**, 2621-2628.